Indian journal of **Engineering**

Simulation model for energy generated in air-cooled condenser assisted by water mist pre-cooling system

Assem Alkarasneh[1*], Waleed Momani[1], Zaid Abulghanam[1,2], Asim H Yousif[2], Alaa Mohammed[2], Omar A Shabi[3], Muntaser Momani[1], Nasser S Bajaba[4], Sayel M Fayyad[1]

To Cite:
Alkarasneh A, Momani W, Abulghanam Z, Yousif AH, Mohammed A, Shabi OA, Momani M, Bajaba NS, Fayyad SM. Simulation model for energy generated in air-cooled condenser assisted by water mist pre-cooling system. *Indian Journal of Engineering*, 2025, 22, e3ije1692
doi: https://doi.org/10.54905/disssi.v22i57.e3ije1692

Author Affiliation:
[1]Department of Mechanical Engineering, Faculty of Engineering Technology Al-Balqa Applied University, Amman, Jordan
[2]Philadelphia University, Jordan
[3]Mechanical Engineering Department, Faculty of Engineering, King Abdulaziz University, Jeddah, Saudi Arabia
[4]Yanbu Industrial College, Saudi Arabia

[*]**Corresponding Author**
Department of Mechanical Engineering, Faculty of Engineering Technology Al-Balqa Applied University, Amman, Jordan
Email: assemalkarasneh@bau.edu.jo

Peer-Review History
Received: 25 August 2024
Reviewed & Revised: 29/August/2024 to 17/January/2025
Accepted: 20 January 2025
Published: 30 January 2025

Peer-Review Model
External peer-review was done through double-blind method.

Indian Journal of Engineering
pISSN 2319–7757; eISSN 2319–7765

DISCOVERY SCIENTIFIC SOCIETY

ABSTRACT

A simulation program for simulating an air-cooled condenser and air conditioning systems is presented in this research. The program can forecast the capacity of a condenser in two scenarios: one involves a clean condenser, and the other involves a condenser which is used in a water mist pre-cooling system. The condensing heat exchange arrangement provided in this study is a cross-flow, aluminum louver fin, unmixed copper tube type, where forced air flows outside the tubes and refrigerant travels inside the tubes. To confirm the accuracy of the mathematical model, experimental studies are also taken into consideration. The components of the test rig set-up are an evaporator, compressor, water mist system, cross flow condenser, open duct air supply, and measuring instruments. The estimated parameters for both cases accord exceptionally well with the projected results of the airflow and refrigerant properties for the air conditioning unit. The A/C unit's performance shows a reasonable degree of consistency between the experimental and forecasted results.

Keywords: Air-Cooled Condenser, Water Mist, Energy, Atomization Nozzle, Condenser Capacity, Coefficient of Performance.

1. INTRODUCTION

In a refrigeration system, a much lower temperature is achieved and maintained for some product or space to be cooled compared to the surrounding environment (Dossat and Horan, 2005). Due to the extreme ambient summer conditions (represented by the high dry bulb temperatures), the overall performance of the refrigeration system is dropped. Water mist pre-cooling can enhance the air-cooled condenser capacity and the coefficient of performance (COP) of the A/C unit. The Mathematical model was used to evaluate the air-cooled condenser capacity and performance. Hamilton and Miller, (1990) developed a general steady-state model for simulating an air-conditioning system. Joudi and Namik, (2003) theoretically studied the component matching the mixed vapor compression system.

A thorough and precise condenser model was developed by Stewart, (2003) and it was paired with a strict model of the entire air conditioning system. Developed a computer program to simulate the working and performance of an air-conditioning window-type system, which consists of four main parts (compressor, condenser, capillary tube, and evaporator), using R-22 as the working refrigerant. Domanski and Yashar, (2007) presented a model for an optimization method to specify a circuit design that maximized the coil capacity using an intelligent optimization method. Yang et al., (2009) demonstrated how pre-cooling the outside air reaching the condenser unit with water mist can increase chiller performance by lowering compressor power. Yu and Chan, (2011) used mist pre-cooling to enhance the COP of an air-cooled chiller system to lower the dry bulb temperature of the outside air.

Chan et al., (2011) reported that (COP) of air-cooled chillers can be improved by adopting variable condensing set point temperature control and using mist evaporation to pre-cool ambient air entering the condensers to trigger a lower condensing temperature. Yang et al., (2012) considered how running a water mist system could improve the thermal performance of chillers with air cooling in various operating scenarios. Considered how the thermal performance can be improved, as the power usage of the compressor is reduced, and the cooling capacity is increased when the water mist device is used in conjunction with the air-cooled conditioner to pre-cool the condenser air that is coming in. The cooling efficiency of a water mist-assisted air conditioner has been investigated experimentally in a temperature range of 20 to 52 degrees Celsius.

Amer et al., (2015) reviewed the recent developments concerning evaporative cooling technologies that could potentially provide sufficient cooling comfort, reduce environmental impact, and lower energy consumption in buildings. An extensive literature review mapped out the state-of-the-art evaporative cooling systems. To maximize cooling capacity and reduce compressor power consumption, Torgal et al., (2016) explained how the performance can be improved when the water mist system is combined using the air-cooled conditioner to pre-cool the air entering the condenser. Soylu et al., (2016) assessed air-cooled chillers with evaporative-cooled condensers, and the evaporative cooling effectiveness on the performance of air-cooled chillers was also investigated.

Yu et al., (2018) presented theoretical and experimental evaluations on how well mist cools an air-cooled chiller, increasing its coefficient of performance (COP). Heidarinejad et al., (2019) examined how a water mist system affects the chiller coefficient of performance (COP) in different spray nozzle orientations. Additionally, a sensitivity analysis is carried out for various ambient air factors, such as air velocity, air temperature, and air humidity ratio. Park et al., (2022) provided the optimal water spray amount for the water mist system, considering the corrosion and cooling effects based on the surrounding temperature, and it applies to commercial procedures. Kaneesamkandi et al., (2023) determined which of the four condenser cooling techniques affect the vapor absorption refrigeration system's performance for effective cooling.

This investigation has aimed to introduce a mathematical model that can predict the capacity and the functionality of an air-cooled condenser which is connected to a pre-cooling system using water mist that assisted the capacity of the air-cooled condenser. The structure of this paper is organized as follows: Section II provides the related theoretical background, the water mist simulation model, heat transport correlations, and the thermodynamics model of the condenser heat exchanger. Section III provides the experimental setup, methodology of study and experimental procedure. The complete results and analyses are explained and discussed in Section IV. Conclusions of the present work are presented in Section V. The work is accomplished by many graphs, tables, figures and an updated reference list.

2. THEORETICAL BACKGROUND

Thermodynamics Model of the condenser heat exchanger

The schematic diagram of the heat exchanger set-up, which depicts the intake and exit of tube circuits to replicate the current condenser, is shown in (Figure 1). The rated power of the condenser used is about (2700 W). The equilibrium of energy in each of these circuits, as shown in Figure (1), results in the following equation:

$$Q_{cr} = \dot{m}_{cr}(h_{in} - h_{out}) \quad (1)$$

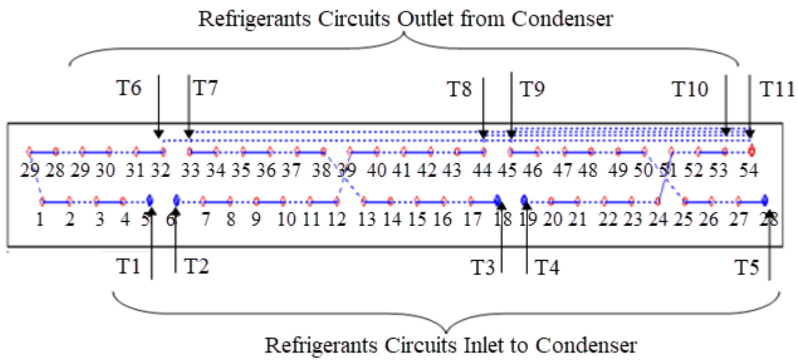

Figure 1 Condenser pipes arrangement layout.

Three portions comprise the condenser: the sub-cooled zone, the saturated (two-phase zone), and the superheated (de-superheating zone). Figure 2 states that the following set of equations can be obtained from an energy balance in each of these sections:

$$q_{cond-sc} = h_{2b} - h_3 \quad (2)$$
$$q_{cond-sh} = h_2 - h_{2a}$$
$$q_{cond-tp} = h_{2a} - h_{2b}$$

Where: the heat transfer per unit mass for the subcooled, two-phase, and superheated regions is denoted by the qcond-sc, qcond-sh, and qcond-tp, respectively.

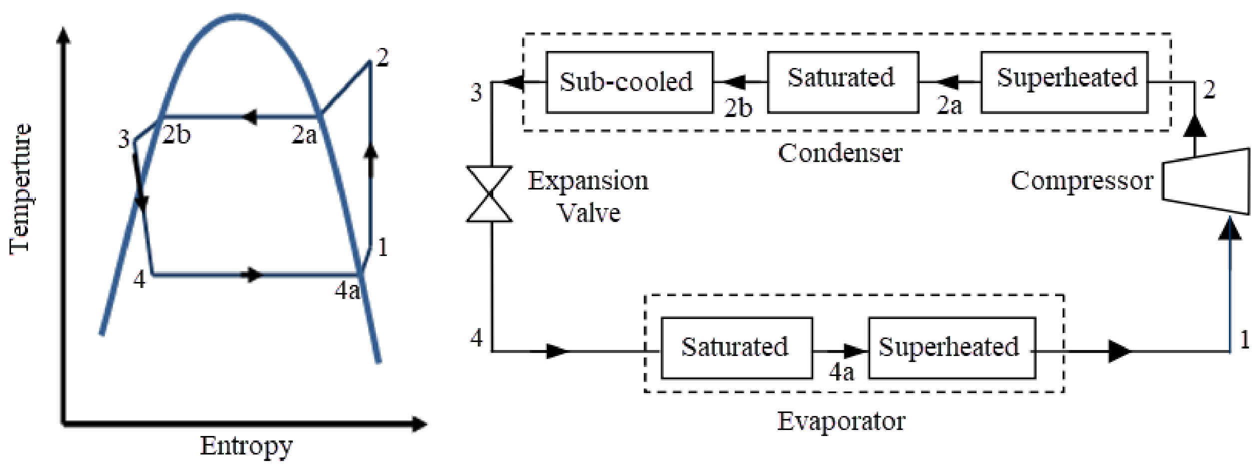

Figure 2 Vapor compression refrigeration cycle

The separate lengths of each segment of the heat exchanger, weighted by the overall tube length in the condenser, can be used to relate the air-side effective mass flow rates over each sector (Stewart, 2003):

$$L_{tot} = L_{sh} + L_{tp} + L_{sc} \quad (3)$$

The effectiveness (ε) of the heat exchanger, the minimum heat capacity (Cmin) of the air or refrigerant side, and the temperature differential between the two fluids' inlets can be used to define the overall heat transfer rate (ASHRAE Fundamental, 1997).

$$Q_{H.E} = \varepsilon . C_{min} . (T_{hin} - T_{cin}) \quad (4)$$

The following equation can be used to calculate the effectiveness of heat exchanger which is defined as the ratio of actual heat transfer to maximum possible heat transfer.

$$\varepsilon = \frac{Q_{H.E}}{Q_{max}} \varepsilon = \frac{Q_{H.E}}{Q_{max}} \quad (5)$$

$$NTU = \frac{UA}{C_{min}}\, NTU = \frac{UA}{C_{min}} \quad (6)$$

In this case, (UA) indicates the product of the heat transfer area (A) and the overall heat transfer coefficient (U). However, in the sub-cooled and saturated zones, the counter-flow effect is ignored because more than 75 percent of the condenser runs in the two-phase region. Due to the lack of analytical correlations for the cross-counter-flow configuration, only cross-flow relations can be applied. The unmixed-unmixed crossflow arrangement is used as the basis for the computations.

By using the model for dry coils given in McQuiston et al., (2023), the air-side convective heat transfer coefficient is calculated for a louvered finned-tube heat exchanger with two rows of staggered tubes. The Colburn j-factor, which is defined in Wang et al., (1999) serves as the foundation for calculating the heat transfer coefficient.

$$j = St.Pr^{\frac{2}{3}} \quad (7)$$

The air-side convective heat transfer coefficient($\overline{h_a}$) is described by the following relationship when the appropriate values are substituted for the Stanton number (St).

$$\overline{h_a} = \frac{j.cp_a.G_{a,max}}{Pr^{\frac{2}{3}}} \quad (8)$$

Where:

$$G_{a,max} = \frac{\dot{m}_a}{A_{min}} \quad (9)$$

To calculate the finned-tube heat exchanger's overall air-side surface efficiency, the first step is to compute the fin's efficiency around a single tube. The second step is calculating the air-side surface efficiency ($\eta_{s,a}$) of a louvered finned-tube heat exchanger with two rows of staggered tubes (Incropera et al., 1996).

Fins area (Afin) and pipes area (Ap) are described with concerning to the schematic diagram (front and side view) of the condenser as seen in Figure (3), where:

The total number of tubes Np is explained according to Shah's method (Shah and Sekulic, 2003):

$$N_P = \frac{L_2 . L_3}{X_T X_L} \quad (10)$$

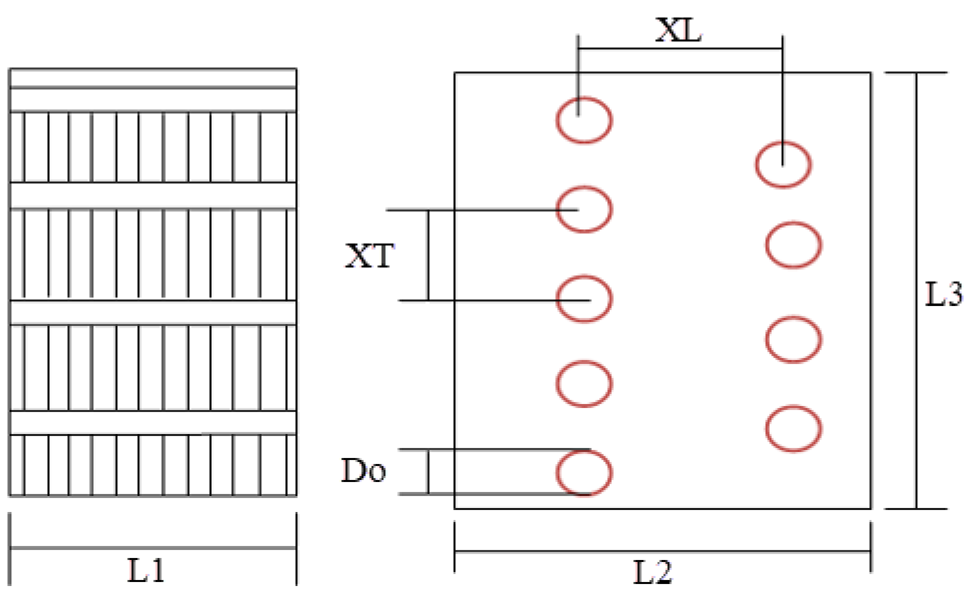

Figure 3 Schematic diagram of the condenser

Heat Transfer Correlation

The formula of heat transfer correlation for single-phase turbulent flow regions (Sub-Cooled and superheated) developed by Kays and London, (2018) is used in the model.

$$St.Pr^{\frac{2}{3}} = a_{st}.Re_{Di}{}^{b_{st}} \quad (11)$$

Where the coefficients a_{st} and b_{st} are given in Table (1).

The Stanton number (St) is expressed as:

$$St = \frac{Nu_D}{Re_{Di}.Pr} = \frac{h_r}{G_{r}.C_p} \quad (12)$$

$$\underline{h}_r = St\ .G_r\ .C_p \quad (13)$$

For the two-phase portion of the condenser, the Shah's correlation has been used (Shah, 1979).

The total pressure drop in the refrigerant side is the summation of the friction pressure drop, the momentum pressure drop, bends pressure drop as well as the gravity pressure drop which is neglected.

$$\Delta P_{tot} = \Delta P_{frication} + \Delta P_{mom} + \Delta P_{bends} \quad (14)$$

The Darcy equation is used to determine the friction pressure drop on the refrigerant side in the single-phase regions (Bruce and Donald, 2002):

$$\Delta P_{frication} = 2.f.\frac{L}{D_i}\frac{G^2}{\rho_I} \quad (15)$$

So, the friction factor found from (Dobson, 1994):

$f = 0.046\ Re^{-0.2}$ For liquid phase

$f = 0.079.Re^{-0.25}$ For gas phase

For bends friction pressure drop [18]:

$$\Delta P_{bends} = f * \frac{G^2}{2.\rho_i} * \frac{L_{bends}}{D_i} * N_{bends} \quad (16)$$

L_{bends} : The length of the bends.

$$L_{bends} = \frac{\pi.X_T}{2}$$

And the momentum pressure drop is calculated from the following equation (Traviss, 1972):

$$\Delta P_{mom} = \frac{-G^2.\left(\frac{1}{\rho_o} - \frac{1}{\rho_i}\right)}{L} \quad (17)$$

The total pressure drop fraction in the saturated region can be estimated by calculating (ΔP_{mom-tp}, $\Delta P_{frication-tp}$ and $\Delta P_{bends-tp}$ as a function of pressure drop friction (x)).

Water Mist Simulation model

The ambient air and mist water mixture humidity (W') can be calculated at a specific dry bulb temperature and air's relative humidity, according to the procedure of calculation given by (ASHRAE Fundamental, 1997) in which:

$$W' = W + \Delta W \quad (18)$$

Where ΔW is the additional air humidity ratio (kg per kg dry air), therefore:

$$\Delta W = \frac{\dot{m}_{mist}}{\rho_a\ .V_a} \quad (19)$$

$$V_a = \frac{R_a.T_a}{P_a} = \frac{R_a.T_a}{P_B - P} \quad (20)$$

$$W = \frac{m_s}{m_a} = 0.622\frac{P}{P_B - P} \quad (21)$$

Here, (P) refers the partial pressure of water vapor. (P_B) denotes to the barometric pressure and (p) can be found as:

$$P = P_{sw} - P_B.A.(T_D - T_W) \quad (22)$$

Where (A) is constant given by:

$$A = 6.66 * 10^{-4}\, C^{-1} \quad T_W > 0°C$$
$$A = 5.94 * 10^{-4}\, C^{-1} \quad T_W < 0°C$$

Based on (ASHRAE Fundamental, 1997) the specific enthalpy of the wet air is constant because the evaporation of water mist into the air is adiabatic.

$$h = 1.007\, T_D - 0.026 + W'(2501.3 + 1.84\, T_D) \tag{23}$$

Additionally, the temperature of the condenser air T_{cae} that is entering can be computed as follows:

$$T_{cae} = \left(\frac{h - (2501.3 * W')}{1.007 + (1.84 * W')}\right) - 0.026 \tag{24}$$

The relative humidity Ø is a function of the degree of saturation (μ) and can be calculated as follows:

$$Ø = \frac{\mu}{\left(1 - (1 - \mu) * \left(\frac{P_{sw}}{P}\right)\right)} \tag{25}$$

Where: (P_w) is the partial pressure of water vapor in the air stream at the given temperature (T_{cae}). And (μ) is the degree of saturation (the ratio of air humidity ratio (W) to humidity ratio of saturated moist air (W_S) at the same temperature and pressure), therefore:

$$\mu = \frac{W}{W_S}|_{T,P} \tag{26}$$

and

$$W = \frac{(2501 - 2.326 * T_W) * T_W - 1.006 * (T_{cae} - T_W)}{(2501 + 1.86 * T_{cae}) - (4.186 * T_W)} \tag{27}$$

Before calculating the relative humidity (Ø) of the air at the inlet of the condenser coil, the air humidity ratio (W) and the saturated air humidity ratio (W_S) have to be determined first. The air humidity ratio (W) at the temperature of the air at the condenser inlet (T_{cae}) can be calculated by using Eq. (27). (W_S) at (T_{cae}) can be calculated using equations (21) and (22). If the calculated humidity ratio (W) is higher than the maximum allowable humidity ratio at the saturation state (Ø ≥1), the air at the inlet of condenser becomes saturation, and (T_{cae}) becomes equal to wet-bulb temperature (T_W).

Under such conditions, the water mist generation rate is more than needed. From Eq. (20), the amount of water evaporated and change of the humidity ratio are linked to the air velocity moving through the condenser coil, hence, (T_{cae}) at the inlet of condenser is affected by the air velocity. The condenser performance and capacity calculation and water mist procedure calculation are programmed by MATLAB. The input data of thermal parameters of refrigerant and ambient air to the program is the same as that of experimental and the actual condenser circuits and tube arrangement and dimensions. Table 1 shows condenser dimensions.

Table 1 Condenser and circuit dimensions

Transverse (vertical) tube spacing (XT), (mm)	12.27
Longitudinal (horizontal) tube spacing (XL), (mm)	22
Inside tube diameter, (Di), (mm)	6.2992
Outside tube diameter (Do), (mm)	7.9248
No. of circuits	5
Ltot, (m)	49.28
Lc1, (m)	10.2054
Lc2, (m)	10.05816
Lc3, (m)	10.19313
Lc4, (m)	6.64
Lc5, (m)	8.38589

Experimental Background

Experimental Setup

The schematic diagram of the test rig is shown at (Figure 4). The room that contains the indoor unit is occupied with electrical heaters to balance the cooling load. Refrigerant (R22) is the working fluid of the A/C unit. The thermodynamic properties of R22 are taken from standard ASHRAE tables.

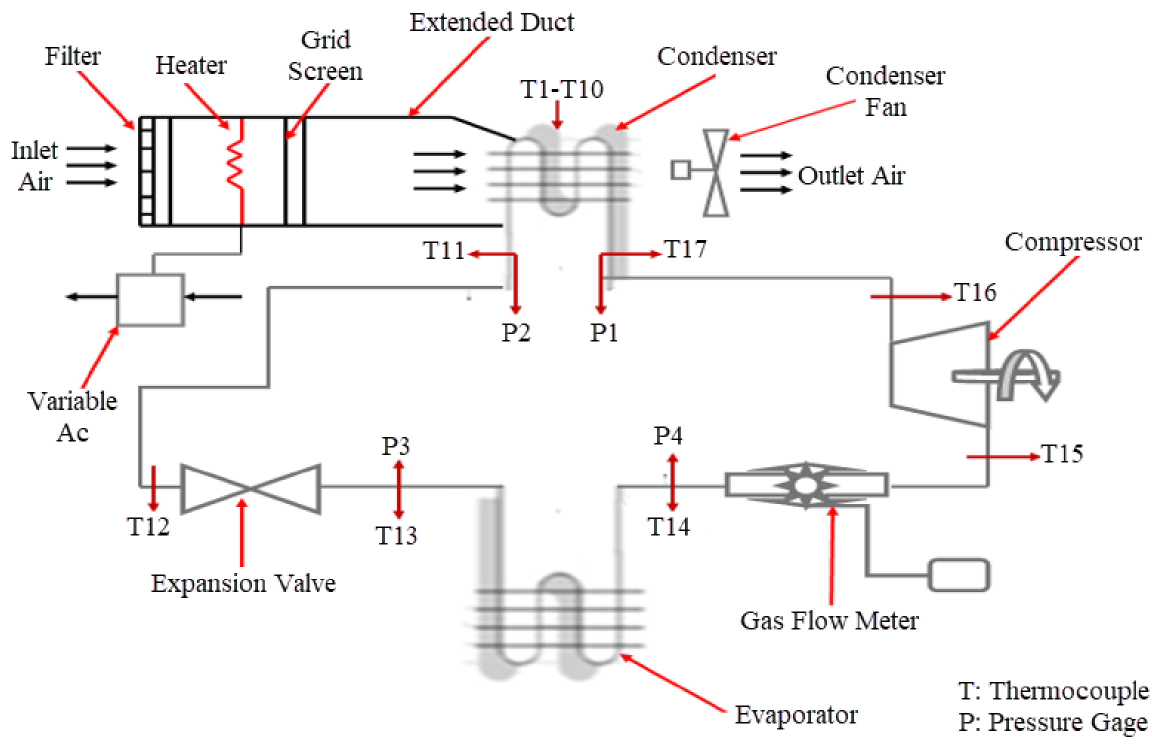

Figure 4 Test rig setup & arrangement

The schematic diagram of the water mist system is shown in (Figure 5). The system consists of a displacement electrical pump, filter, atomization nozzle, and tubes. The atomization nozzle is located at the extended duct before the condenser. Distilled water is sent to the pump at a pressure of about 30 bars. The atomization nozzle gives fine droplets of (5μm).

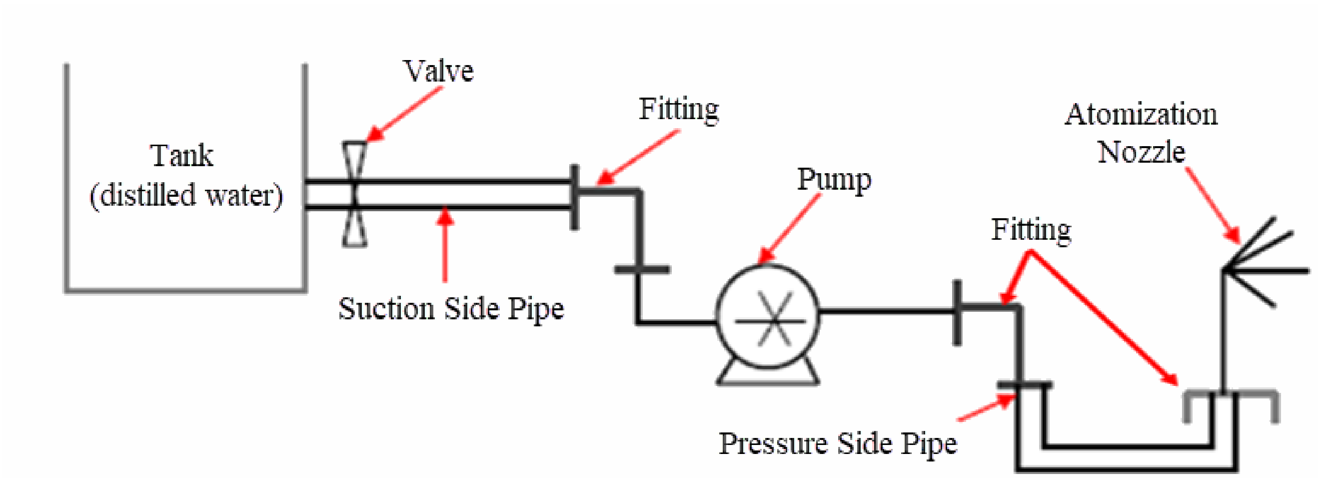

Figure 5 System of water mist

The open duct is designed to fit the air side of the condenser intake. The dimensions and the geometry of the duct are shown schematically in (Figure 6). The laboratory experimental temperature (ambient air drawn by the outdoor unit fan) is ranging between (35˚C) and (48˚C).

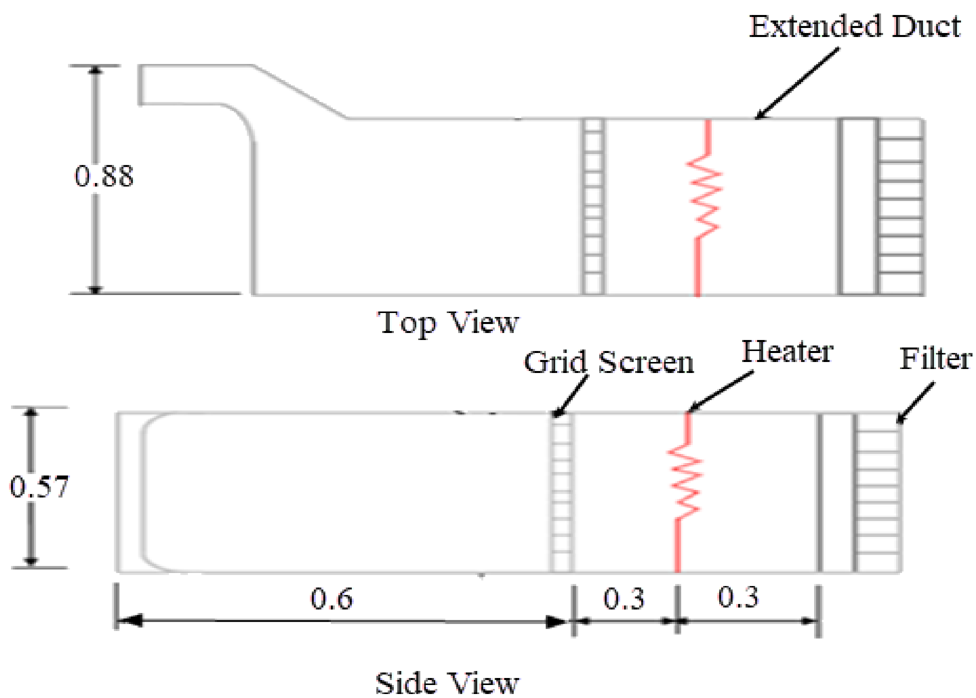

Figure 6 Extended air duct

These temperatures can be achieved during all seasons by using an electrical heater. The duct contains filter at the duct entrance, electrical heater and grid screen. Therefore, the dry and wet bulb temperatures of the air are continuously monitored at the exit of the duct, i.e., at the inlet of the condenser. To minimize the heat losses to the surrounding, the duct was insulated completely. The measuring devices used in the present work are (17 thermocouples type K (TP-01A probe), (4 pressure gages (filled oil Bourdon type (BTC)), KF500 series turbine flow meter, anemometer air flow meter model (YK2005), Humidity meter model (LM-81HT), analog-digital clamp meter model (MT-3266), and data acquisition unit.

In each experimental test, the thermal properties and mass flow rate of the refrigerant are measured. These parameters are refrigerant temperatures in the condenser (inlet and outlet at each circuit (12 points) and refrigerant pressure inlet and outlet to the condenser. The temperature of outside air (inlet/outlet) to the condenser, refrigerant temperature (inlet/outlet) to the evaporator, and refrigerant pressure (inlet/outlet) to the evaporator are also measured. The parameters (air velocity at inlet to the condenser, the power consumed by the compressor and relative humidity before the condenser) are also calculated.

Experimental procedure

The ability to change the mass flow rate of the refrigerant is not available in the A/C unit since the compressor is running at a constant speed. The running speed of the condenser fan is also constant, keeping the air mass flow rate constant. Therefore, the only parameter that affects the performance of the condenser is regarded as the outdoor ambient air temperature, in which the outdoor ambient temperature is considered one of the most critical parameters that affect the condenser capacity. Therefore, the outdoor ambient temperature variation takes standard values of temperature variation as (35, 38, 40, 43 and, 48˚C) during the experimental program test. The program for investigations is designed for two cases, case (1) is for clean condenser while case (2) is for the condenser occupied with a water mist pre-cooling system. Both cases include predicted and tested results.

The mathematical model of the condenser is programmed by MATLAB**.** The input data to the MATLAB program is the measured data obtained from the test rig. The program can compute the dryness fraction (x) of the two-phase flow. The refrigerant side total pressure drop depends widely on the refrigerant dryness fraction (x) of the two-phase flow in condenser pipes. The input data is the coil shape and dimensions as given in Table 1 and the conditions under which the test is operated.

3. RESULTS AND DISCUSSION

Verification of the mathematical model

The expected results of fluid characteristics are compared with the tested results to confirm the reliability and stability of the predicted results derived from the mathematical model. Both results showed a very close condenser refrigerant inlet and outlet properties, as shown in Figures (7, 8, 9, 10, and 11). The maximum order of deviation of refrigerant inlet temperature (discharge temperature), refrigerant outlet temperature, refrigerant inlet enthalpy, refrigerant mass flow rate, and refrigerant inlet pressure are (+0.839, -1.94, +0.29, -2.784, -1.507), respectively.

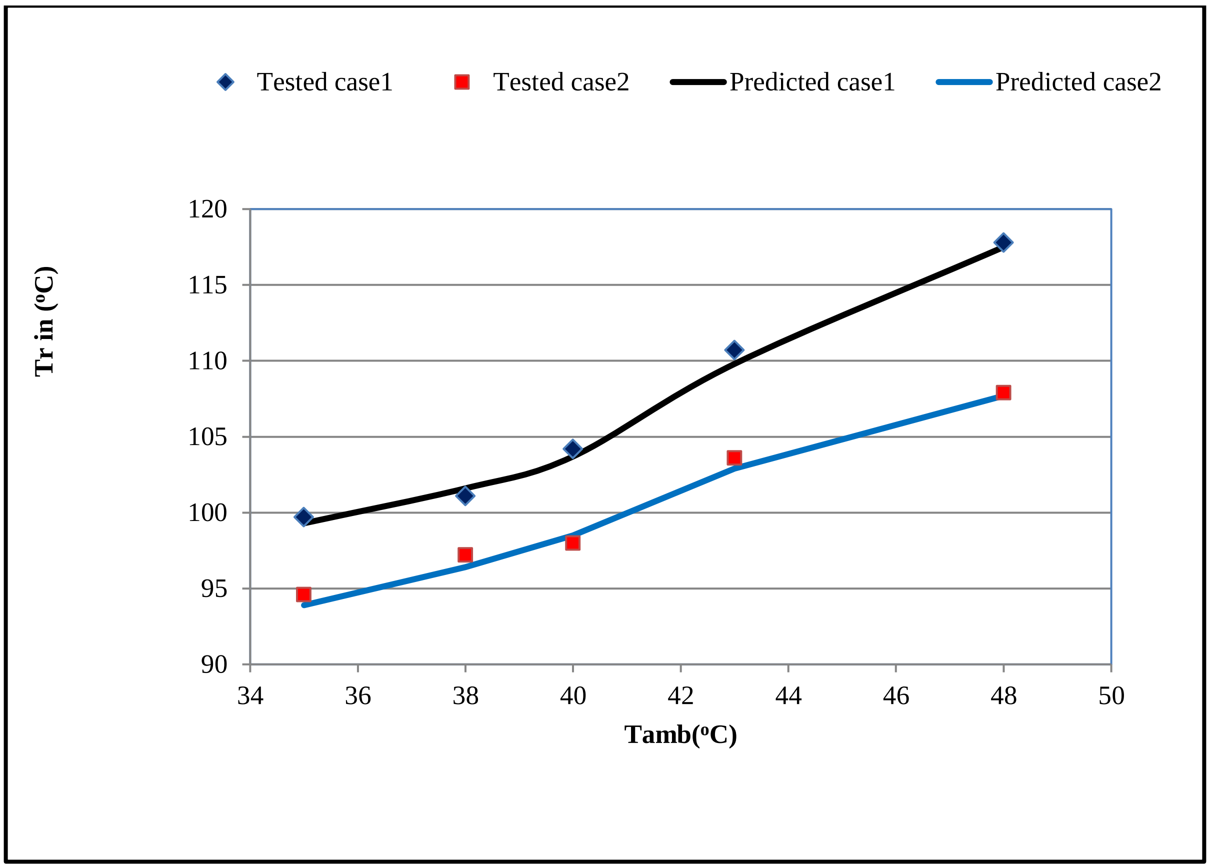

Figure 7 Variation of inlet refrigeration temperatures via ambient air temperature.

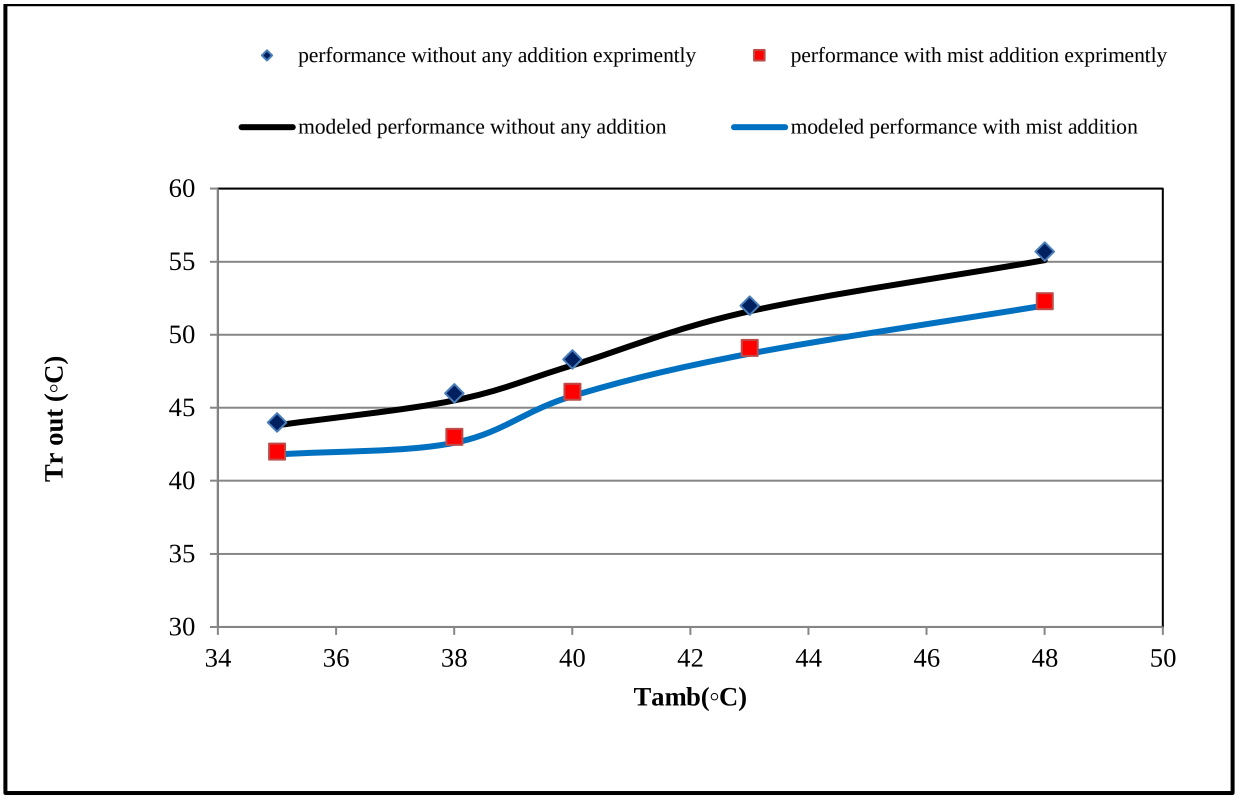

Figure 8 Variation of outlet refrigeration temperatures via ambient air temperature.

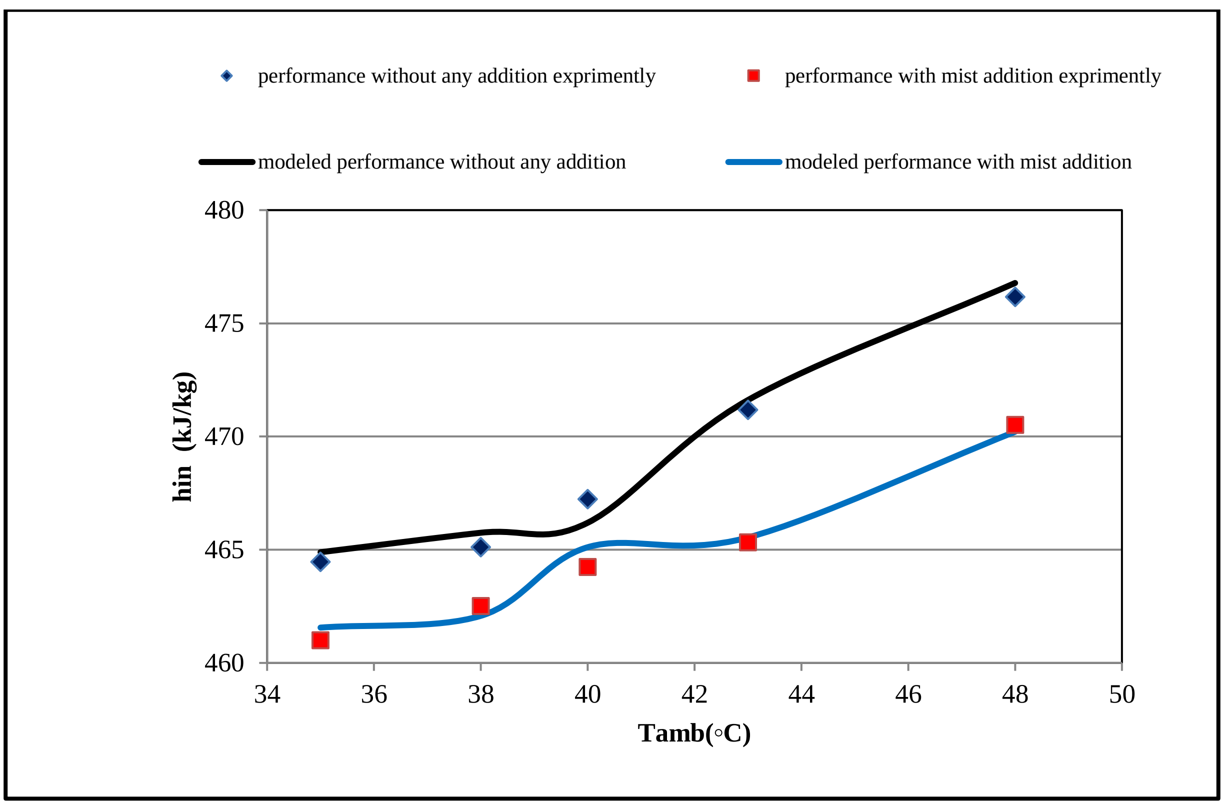

Figure 9 Variation of inlet enthalpy via ambient air temperatures.

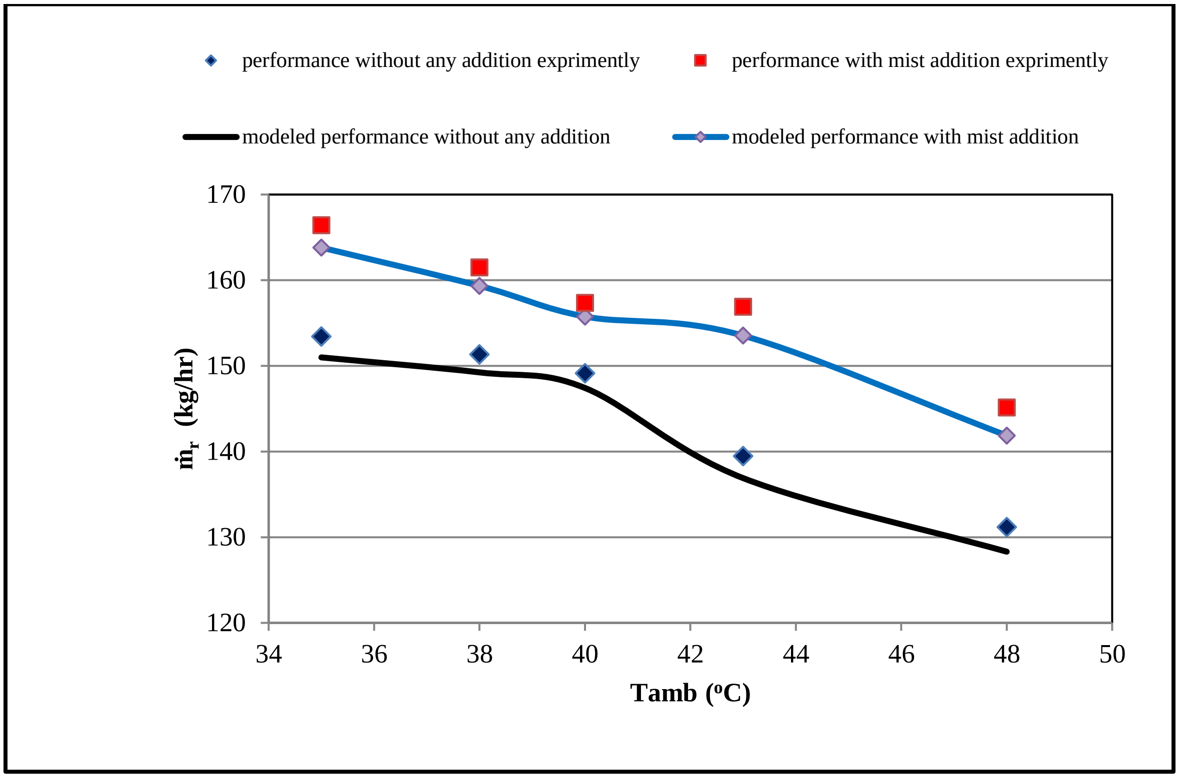

Figure 10 Variation comparison refrigerant mass flow rate via ambient air temperatures.

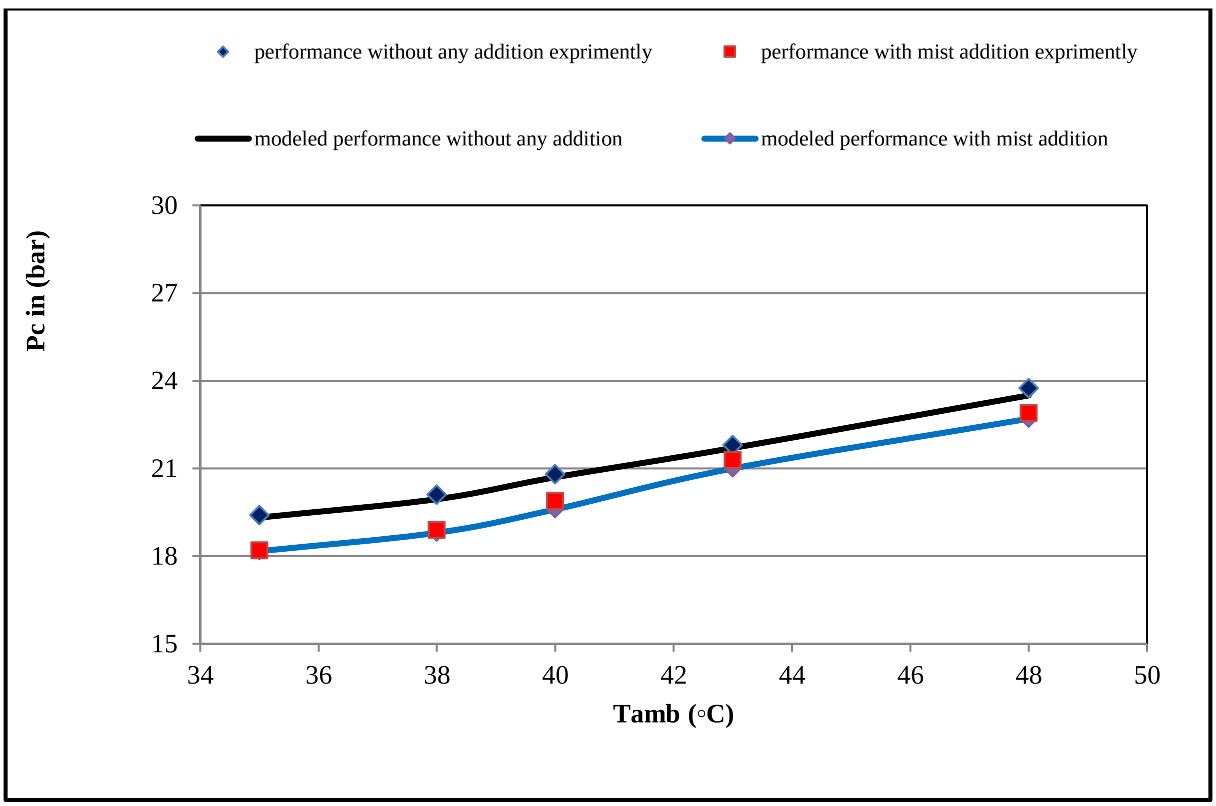

Figure 11 Variation of the inlet condenser pressure via ambient air temperatures.

Measured and predicted showed close values of refrigerant two-phase, super heat and sub-cool flows enthalpies, as shown in Figures (12, 13, 14, and 15). For example, the maximum deviation obtained from all tests in refrigerant two-phase flow enthalpy, refrigerant super heat flow enthalpy, refrigerant sub-cool enthalpy, and refrigerant pressure drop are of order of (-0.1793, -1.902, -0.788, and -1.85), respectively.

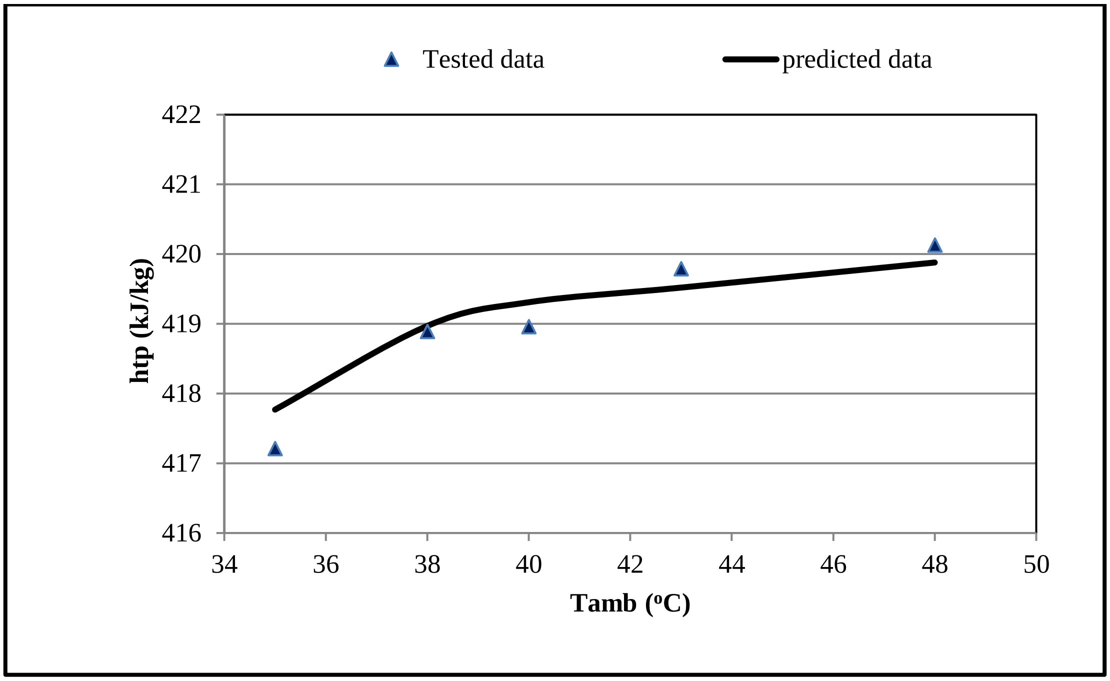

Figure 12 Two phase flow enthalpy variation via ambient air temperature

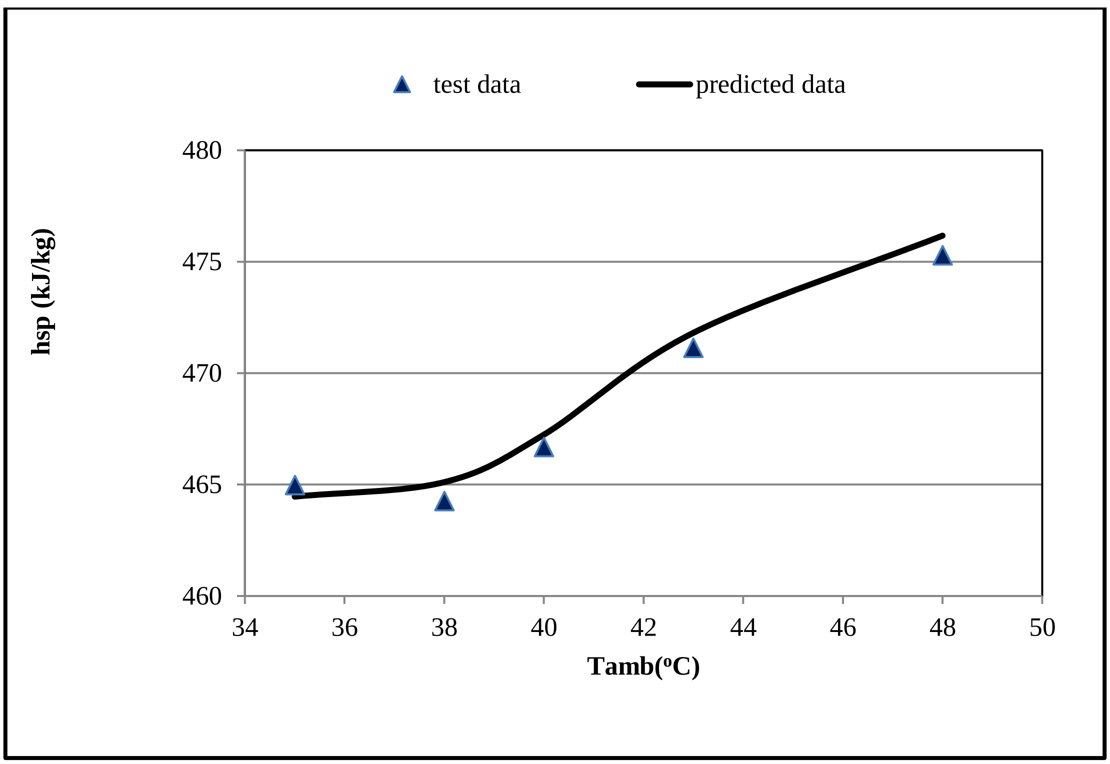

Figure 13 Superheated flow enthalpy variation with ambient air temperatures.

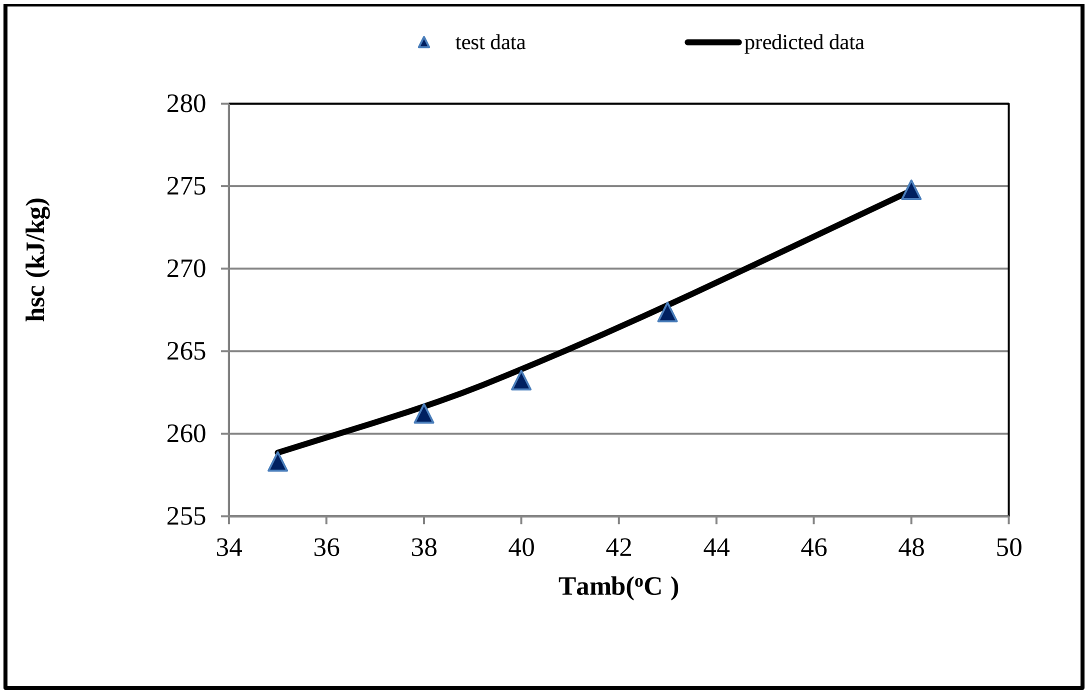

Figure 14 Sub-cooled flow enthalpy variation ambient air temperatures.

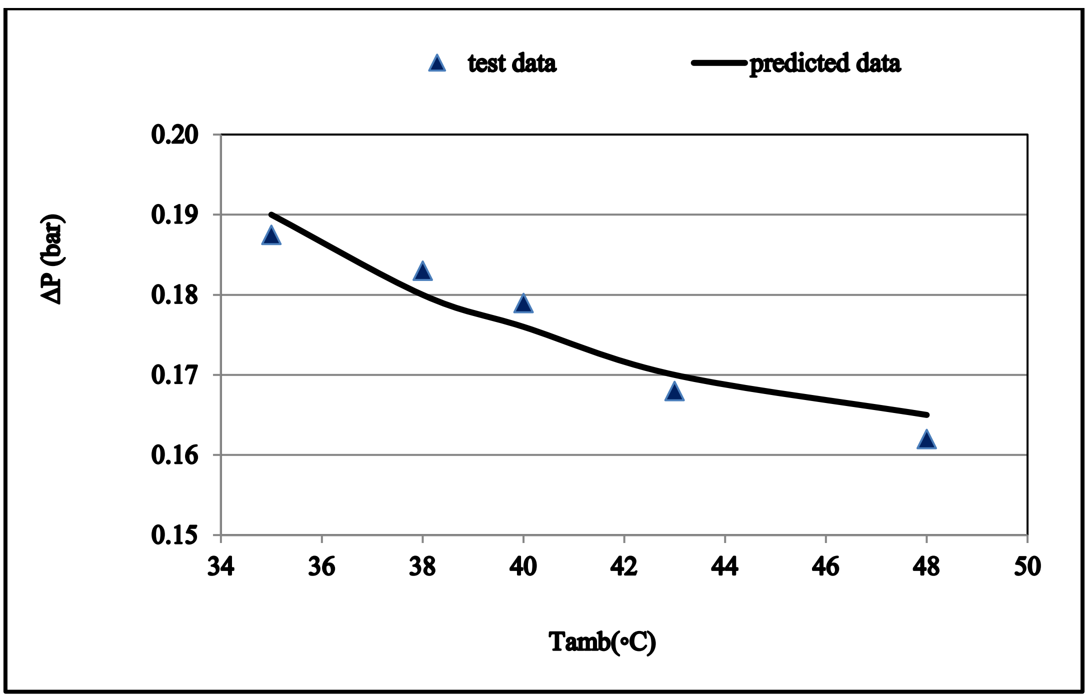

Figure 15 Pressure drop via ambient air temperatures.

Coefficients of performance

In this investigation, the coefficient of performance (C.O.P) was observed to increase by 14.45% at the ambient temperature of 43ºC, as illustrated in Figure 16, because of the increased condenser size capacity. The result corroborates the reported by Jassim, (2014) where the C.O.P was at 8.5% and rose to 17.5% when the air temperature supplied to the condenser was reduced from 52ºC to 20ºC. Despite the similarity of C.O.P improvement trends in both research works, Jassim, (2014) study adopted a wider temperature span, which underscores how different air inlet temperatures can affect system operation. Furthermore, the results of this research are in excellent accordance with those of Birangane and Patil, (2014) also reported the same tendencies in the enhancement of C.O.P.

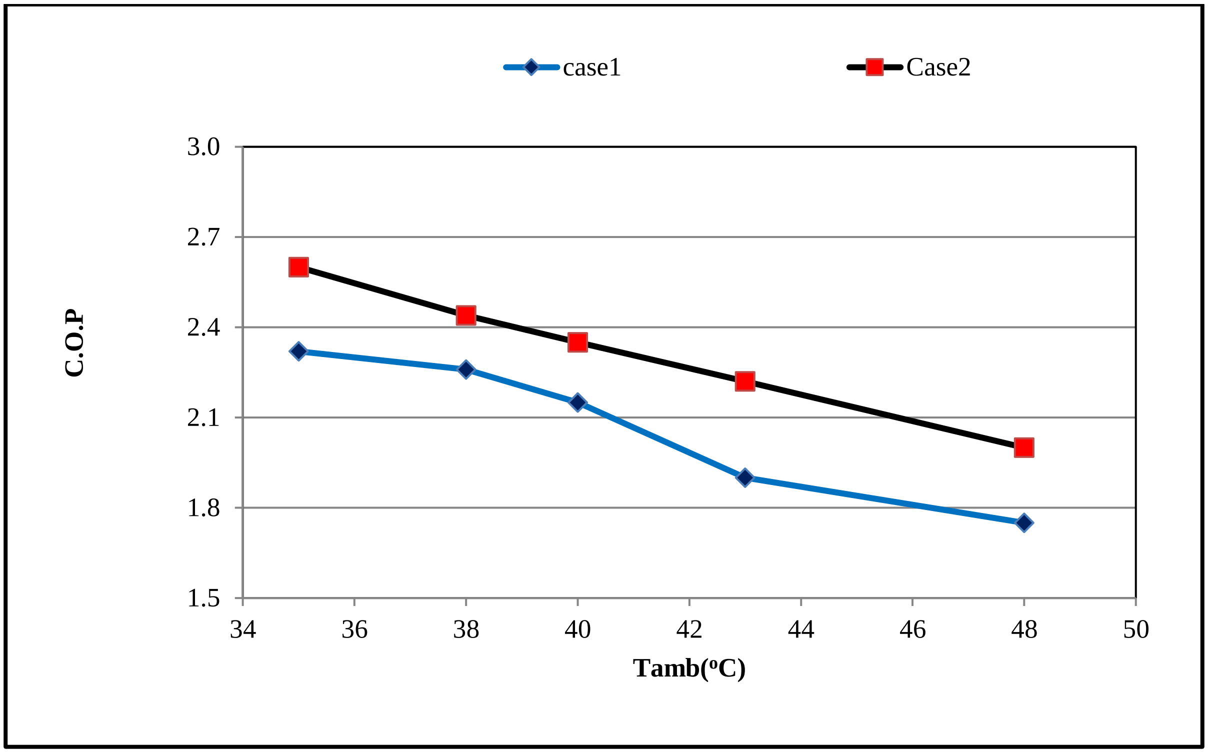

Figure 16 Variation of COP with ambient air temperature

Water mist pre-cooling

The effectiveness of the air conditioner is usually improved by adding water mist, which also changes the characteristics of the surrounding air. As air enters the condenser, its dry bulb temperature drops by (6%) at Tamb=43ºC. As illustrated in Figure 17, the maximum condenser capacity was raised by 9.09% with the application of water mist, concerning to 43ºC ambient conditions. This could be related to the results of Jassim, (2014), where the cooling capacity was enhanced from 8.5% to 17.5%, when the supplied air temperature to the condenser was lowered from 52ºC to 20ºC.

Notably, the performance of the condenser is enhanced in both approaches, however the significant increase in capacity in Jassim, (2014) research stemmed from a broader range of temperature reduction meaning that the air temperature reduction entering the condenser is more effective than the water mist effect at the equivalent conditions. Moreover, the findings provided in this study are consistent with those highlighted by Birangane and Patil, (2014), who observed analogous trends in improving condenser capacity. The refrigerant pressure drop of the ambient air temperature variation for both cases is presented in (Figure 18). For all ambient air temperatures, the refrigerant pressure drop for case two is lower than that for case one.

The calculating relative humidity is increased with a maximum increment of 19.52% at Tamb=43ºC. Accordingly, the refrigerant condensing temperature and pressure decreased and show a maximum decrement of (6.8% and 7.53% at Tamb=43ºC). The water mist pre-cooling system increases the condenser capacity. The compressor work calculated from refrigerant measured pressures and temperatures is increased accordingly, for example compressor work is increased by 0.574% at Tamb=40ºC. As expected, the test measurements of water mist consumption is increased slightly as the ambient air temperatures increased, in which at Tamb=35 C and 48 C the water mist rate is increased from 0.95 l/hr to 0.995 l/hr., this is because air temperature reduction entering the condenser is more effective than the water mist effect at the equivalent conditions and this affects positively the costs by making a considerable reduction in costs and more water availability.

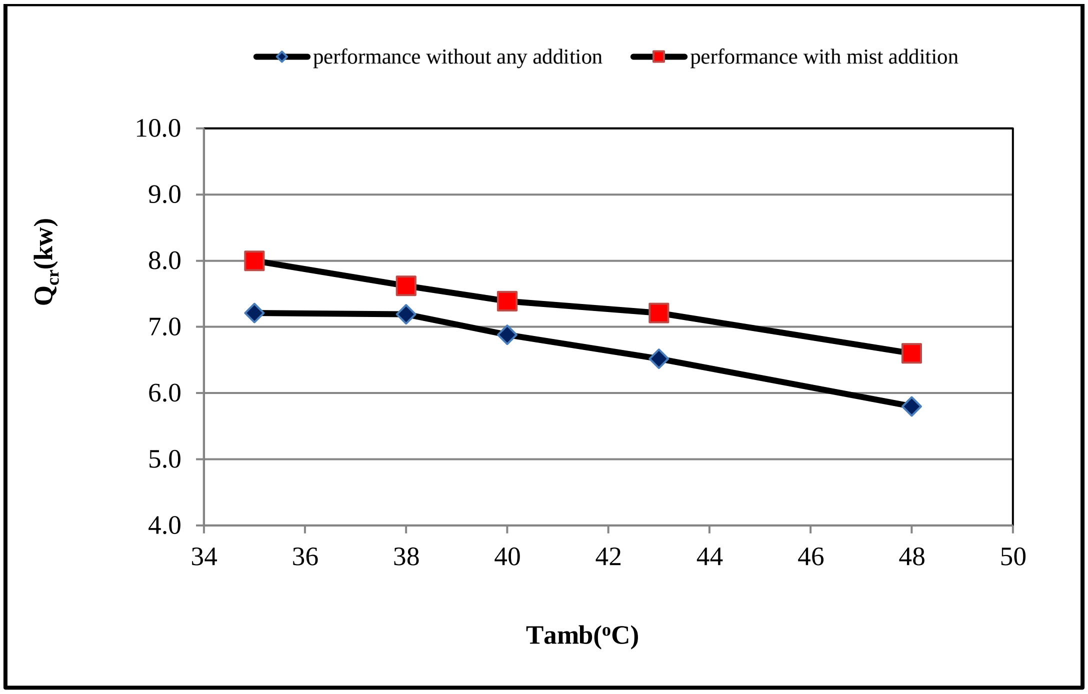

Figure 17 Condenser capacity variation with ambient air temperature.

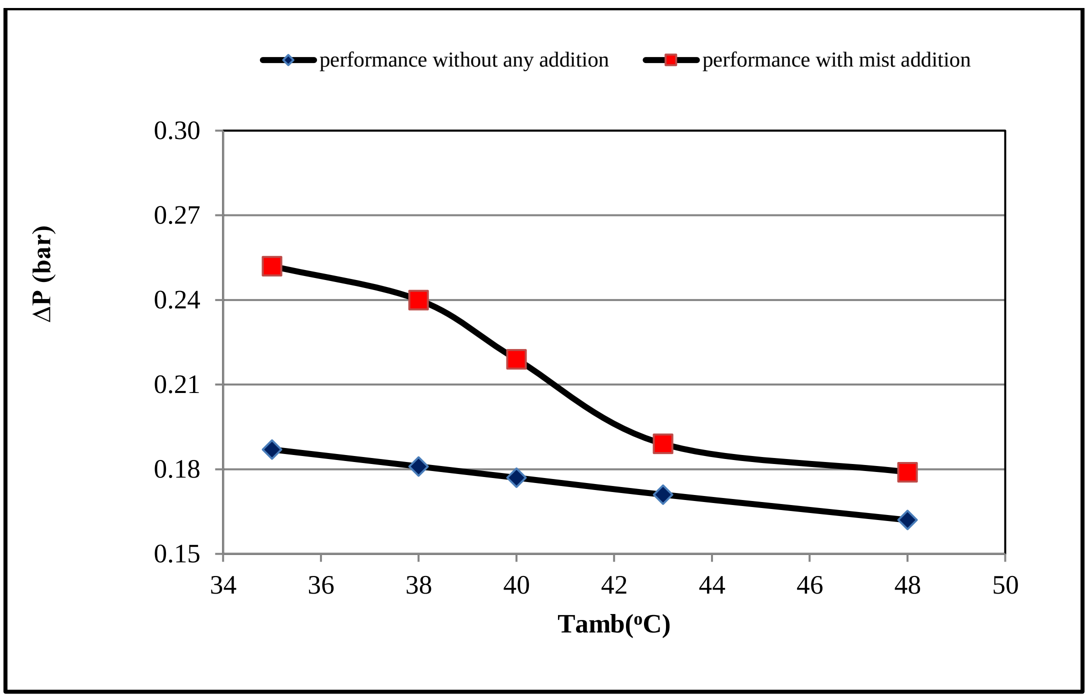

Figure 18 Variation of refrigerant pressure drop via ambient air temperature.

Moreover, the findings provided in this study are consistent with those highlighted in Birangane and Patil, (2014) who observed analogous trends in the improvement of condenser capacity. Compressor work performance was found to increase to 57.4% at 40°C. This has an impact on increasing the overall system energy efficiency and decreasing the operational costs comparing with past literature. The compressor work affects positively on the net energy savings and cost of the water mist pre-cooling system since the performance and COP of the compressor is increased to reach 57.4%. Also, it was noticed that there are effects on environmental implications of water mist systems, such as there is a considerable reduction of water consumption and potential scaling or fouling of condenser coils.

4. CONCLUSIONS

An extraordinarily dependable and practical instrument for assessing the features and performance of condenser heat transfers is the thermodynamic model for air-cooled condensers. To successfully support the validity of the mathematical model, experimental measurements of the fluid and thermal characteristics for the air and refrigerant sides are also employed. The maximum condenser capacity increased by 9.09% and the maximum (COP) by 14.54% at T_{amb}=43ºC and 43ºC, respectively, when the water mist technique was applied. The condenser's ambient air temperature was reduced by 6% when the water mist approach was used.

The condensing temperature and refrigerant pressure are both impacted by this drop in air temperature, decreasing by 6.8% and 7.53%, respectively. Condenser capacity was significantly increased by the water mist approach at 43°K ambient air temperature. During the evaporation process, heat from the air entering the condenser is absorbed by the water mist; latent and sensible heat of the air are also impacted.

Informed consent

Not applicable.

Ethical approval

Not applicable.

Funding

This study has not received any external funding.

Conflict of Interest

The author declares that there are no conflicts of interests.

Data and materials availability

All data associated with this study are present in the paper.

REFERENCES

1. Amer O, Boukhanouf R, Ibrahim HG. A Review of Evaporative Cooling Technologies. Int J Environ Sci Dev 2015; 6(2):111–117. doi: 10.7763/ijesd.2015.v6.571
2. ASHRAE FundamentaL. ASHRAE Fundamentals Handbook. SI, Chapter 27, 1997.
3. Birangane VV, Patil AM. Comparison of Air Cooled and Evaporatively Cooled Refrigerartion Systems–A Review Paper. J Eng Res Appl 2014; 4(6):208-211.
4. Bruce RM, Donald FY. Fundamentals of fluid mechanics. John Wiley & Sons; 2002.
5. Chan K, Yang J, Yu F. Energy performance of chillers with water mist assisted air-cooled condensers. Proceedings of Building Simulation, Sydney, Australia, 2011.
6. Dobson MK, Chato JC, Wattelet JP, Gaibel JA, Ponchner M, Kenney PJ, Shimon RL, Villaneuva TC, Rhines NL, Sweeney KA, Allen DG, Hershberger TT. Heat transfer and flow regimes during condensation in horizontal tubes. Ph.D. thesis, Dept. of Mechanical and Industrial Engineering, University of Illinois at Urbana-Champaign, 1994.
7. Domanski PA, Yashar D. Optimization of finned-tube condensers using an intelligent system. Int J Refrig 2007; 30(3) :482–488. doi: 10.1016/j.ijrefrig.2006.08.013
8. Dossat JR, Horan JT. "Principles of Refrigeration" fifth edition, Wideband Communication Systems, NJ: Prentice Hall PTR, 2005.
9. Hamilton JF, Miller JL. A simulation program for modeling an air-conditioning system. ASHRAE transactions 1990; 96(1):21 3-21.
10. Heidarinejad G, As'adi-Moghaddam MR, Pasdarshahri H. Enhancing COP of an air-cooled chiller with integrating a water mist system to its condenser: Investigating the effect of

spray nozzle orientation. Int J Therm Sci 2019; 137:508–525. doi: 10.1016/j.ijthermalsci.2018.12.013

11. Incropera FP, DeWitt DP, Bergman TL, Lavine AS. Fundamentals of heat and mass transfer. John Wiley & Sons, New York; 1996.
12. Jassim NA. Thermal performance evaluation of water mist assisted air conditioner. Int J Comput Appl 2014; 105(16):5–10.
13. Joudi KA, Namik HNH. Component matching of a simple vapor compression refrigeration system. Energy Convers Manage 2003; 44(6):975–93. doi: 10.1016/s0196-8904(02)00060-2
14. Kaneesamkandi Z, Almujahid A, Salim B, Sayeed A, AlFadda WM. Enhancement of Condenser Performance in Vapor Absorption Refrigeration Systems Operating in Arid Climatic Zones—Selection of Best Option. Energies 2023; 16(21):7416. doi: 10.3390/en16217416
15. Kays WM, London AL. Compact heat exchangers. MEDTECH A scientific International Pvt.Ltd, 2018.
16. McQuiston FC, Parker JD, Spitler JD, Taherian H. Heating, ventilating, and air conditioning: analysis and design. John Wiley & Sons; 2023.
17. Park H, Roh J, Oh KC, Cho H, Kim J. Modeling and optimization of water mist system for effective air-cooled heat exchangers. Int J Heat Mass Transf 2022; 184:122297. doi: 10.1016/j.ijheatmasstransfer.2021.122297
18. Shah MM. A general correlation for heat transfer during film condensation inside pipes. Int J Heat Mass Transf 1979; 22(4): 547–56. doi: 10.1016/0017-9310(79)90058-9
19. Shah RK, Sekulic DP. Fundamentals of heat exchanger design. John Wiley & Sons; 2003.
20. Soylu SK, Atmaca İ, Doğan A. Investigation of evaporative cooling effectiveness on the performance of air–cooled chillers. Online J Sci Technol 2016; 6(3):36-39.
21. Stewart SW. Enhanced finned-tube condenser design and optimization. Georgia Institute of Technology,Atlanta, 2003.
22. Torgal S, Pawar K. Analysis of an air conditioner using both water mist and air for cooling in condenser. Int J Adv Eng Res Sci 2016; 3(5):098-102.
23. Traviss DP. Condensation in refrigeration condensers. Massachusetts Institute of Technology, 1972.
24. Wang CC, Lee CJ, Chang CT, Lin SP. Heat transfer and friction correlation for compact louvered fin-and-tube heat exchangers. Int J Heat Mass Transf 1999; 42(11):1945–1956. doi: 10.1016/s0017-9310(98)00302-0
25. Yang J, Chan K, Wu X. Application of water mist pre-cooling on the air-cooled chillers. Eleventh International IBPSA Conference, Scotland, 2009.
26. Yang J, Chan KT, Wu X, Yu FW, Yang X. An analysis on the energy efficiency of air-cooled chillers with water mist system. Energy Build 2012; 55:273–284. doi: 10.1016/j.enbuild.2012.09.018
27. Yu FW, Chan KT. Improved energy performance of air-cooled chiller system with mist pre-cooling Mist improvement on air-cooled chillers. Appl Therm Eng 2011; 31(4):537–44. doi: 10.1016/j.applthermaleng.2010.10.012
28. Yu FW, Ho WT, Chan KT, Sit RKY. Theoretical and experimental analyses of mist precooling for an air-cooled chiller. Appl Therm Eng 2018; 130:112–119. doi: 10.1016/j.applthermaleng.2017.11.046